

EXPLOITING MELT COMPRESSIBILITY TO ACHIEVE IMPROVED WELD LINE STRENGTHS

David O. Kazmer^{**}, University of Massachusetts Amherst
Department of Mechanical & Industrial Engineering
Engineering Laboratory Building
Amherst, Massachusetts 01003
kazmer@ecs.umass.edu

David S. Roe, Apple Computer Inc.
1 Infinite Loop
Cupertino, California 95014-2084
d.roe@apple.com

^{**} Primary author to whom correspondence should be addressed.

Abstract

The structural integrity of thermoplastic composite parts varies significantly with the local polymer morphology, fiber distribution, and fiber orientation. Reduction of 30% in the ultimate stress and impact properties of knit-lines in composite-filled parts are common, with much greater losses being reported for many material systems [1,2,3]. This paper presents a method for increasing the knit-line strength to or beyond the nominal strength of the part without requiring additional investment in tooling or processing. Moreover, the technique's fundamental concept should lead to additional strategies for dynamically controlling the polymer flow and fiber orientation to deliver maximal part properties for composite material systems.

Introduction

Complex, short fiber composite parts are often manufactured through the injection molding process. In injection molding, knit-lines result when the part is injected via multiple gates and/or when the flow splits as it flows around an obstacle such as a core or pin in the mold cavity. The flow separation causes an inhomogeneity in the polymer's structure due to the disturbance in morphology when the flow splits and then recombines. Often, the part's mechanical strength is reduced in areas where knit-lines occur as a direct result of the localized change in the morphology of the polymer molecular structure [1, 4-5]. Cloud and McDowell characterized knit-line strengths in tensile specimens, reporting 30 to 50% loss in the ultimate tensile stress for common material systems such as polycarbonate and Nylon 66 resins with 10% to 30% glass fiber [2].

The formation of a knit-line where two flow fronts directly impinge upon one another has been defined as a class 1 knit-line [6]. When the polymer flow is split by an

obstacle and then immediately rejoined, the resultant knit-line is designated as class 2. Class 1 and 2 knit-lines exhibit different characteristics because the resultant orientation and morphology at their interface differs. With class 2 knit-lines the velocity, viscosity, temperature, and time with which the knit-line is formed changes as a function of length over which the two flows weld together. In the injection molding process, the mechanical properties of the knit-line will depend upon the temperature, pressures, velocity, and the viscosity with which the two converging flows weld together. The intensity with which the two flows meet, coupled with the amount of diffusion and orientation of the polymers' molecular chain segments across the interface, will directly effect the mechanical properties of the knit-line. Unfortunately, the knit-line location usually becomes an axis of symmetry for the cavity pressure distribution due to flow behavior. As such, no material or fiber convection occurs across the knit-line interface and only a few chain segments diffuse across the boundary.

The decrease in the mechanical properties at the knit-line is directly related to the orientation of the molecular chain segments and composite fibers in this region. The only forces holding the two flow fronts together are secondary forces or Van der Waals forces and any chain entanglements which occurred across the knit-line interface due to diffusion. Polymeric materials are primarily composed of carbon-carbon backbones. The decrease in strength can be explained by comparing the forces which hold the primary carbon-carbon bonds to the strength of the secondary forces. The force required to separate a carbon-carbon bond is 83 Kcal/mol; the force required to break a Van der Waals bond is 2-5 Kcal/mol [7]. Additionally, as the flow proceeds through the cavity, it displaces the air in front of the melt flow. Even if adequate venting is provided in the mold cavity, the two

flow fronts must displace the air between them when they meet. This air displacement results in a formation of vee-notches at the surface of the molding that will reduce the mechanical properties of the part. Hagerman [6] polished out vee-notches in ABS samples to show higher and more consistent tensile strength than in the original unpolished samples.

These three primary factors – poor bonding/adhesion, orientation, and vee notching – are illustrated in Figure 1, a rendering of the knit-lines cross section through the thickness [8]. In Figure 1, the molecular and fiber orientation is represented by the aspect ratio of the ellipses. Away from the knit-line, flow-induced shear stresses will tend to orient composite fibers in the direction of the polymer flow. At the knit-line, however, there is negligible convective flow and shear stress to drive orientation or melt diffusion which results in a fairly random orientation at the knit-line. Analytical models have been developed and validated for the prediction of fiber orientation and part strength [9, 10]. When knit-line difficulties arise in composite filled parts, molders often attempt to resolve the issue by increasing melt/mold temperature and/or hold pressure/time to provide greater molecular diffusion across the interface and subsequently enhanced knit-line strength. Unfortunately, there are many applications for which molding process changes alone can not provide adequate product properties. For these cases, the product must be redesigned to move the knit-line location, or utilize different material systems.

Recently, techniques have been introduced to provide new solutions to increasing the knit-line strength [11-15]. In these approaches, the molten material near the knit-line is subjected to a pressure gradient across the weld interface. This pressure differential drives material flow across the knit-line interface which enhances the chain diffusion and bonding

as well as the local orientation. For instance, Malloy et. al. [12] utilized a multi-live feed injection molding process to drive post-filling phase fluid flow during the packing and solidification of the cavity. The resultant molded part demonstrated weld-line strength equal to the strength of molding produced without knit-lines. Similarly, Michaeli et. al. utilized a push-pull technique to achieve flow across the knit-line [13]. Using a different processing paradigm, Dooley [14] induced transient flow across the knit-line by opening an empty section of the cavity after fill. Also, Garder and Cross were able to generate knit-line diffusion by oscillating ejector pins in the vicinity of the weld line [15].

The anticipated effect of the melt forcing is shown in Figure 2, which results in knit-line strengths of the molded product approaching that of the nominal part (without knit-lines) in the majority of these studies. The resulting polymer flow across the weld interface increases the molded part properties for several reasons. First, convection of the melt across the knit-line interface results in significant molecular transport, diffusion, and generation of carbon-carbon bonds. Fiber distribution and orientation would likewise be increased across the flow direction, resulting in significant increases in composite parts. Finally, there have been claims of significant viscous heat generation and elimination of the vee-notches on the surface of the part, but these effects remain to be sufficiently validated.

Using analytical techniques which have been described [9-10, 16-17], it is possible to predict the strength of knit-lines given post-filling melt convection. This article introduces a technique for increasing knit-line strength similar to the multi-live feed and push-pull techniques previously mentioned. However, this technique does not require any instrumentation beyond a conventional hot manifold with valve gates, which are prevalent

in the plastics industry. To induce flow across the knit-line this process relies upon a property inherent to all thermoplastics – compressibility.

Analysis

Compressibility is an inherent property of thermoplastics, stemming from the free volume surrounding the molecules in the polymer matrix. The physics and effects of compressibility in the injection molding process have been well modeled and clearly illustrated through computer simulation [17-20]. Figure 3 provides observed data for the pressure-specific volume-temperature (PvT) relationship for a 20% glass filled, high flow grade of amorphous polycarbonate. Typically, polymeric materials undergo temperature and pressure fluctuations as they are (a) plasticized, (b) injected, (c) pressurized, and (d) solidified in the cavity. These events are identified by the symbols on the graph with corresponding conditions shown in Table 1.

It should be noted that the maximum change in specific volume which may be induced during the injection and packing stages occurs between the melt at a high temperature and low pressure condition (point A in Figure 3) and melt at low temperature and high pressure condition (point D). These conditions correspond to melt in the barrel before injection and frozen material in the mold at the end of the holding stage, respectively. Between these two conditions, the change in melt specific volume is approximately 10%.

The proposed process for increasing knit-line strength begins with conventional filling of the mold cavity with all valve gates open to permit a balanced fill. Then, one gate is fully closed while the injection unit maintains high pressure at the nozzle. This causes the melt to compress throughout the cavity and drive flow across the knit-line

towards the closed gate as shown in Figure 2. The pressure is maintained while the part begins solidification and the knit-line is further deformed towards the closed gate. At a later time, the open and closed gates are reversed. Additional cycles may be repeated several times which the conventional packing and cooling stages then follow. The pressure and gate sequences are illustrated in Figure 4.

To quantify the magnitude of melt displacement using this technique, a process model of the packing stage was developed for a cross section of the part between two valve gates. This analysis begins immediately after the filling stage is completed and assumes a uniform melt temperature throughout the part. This assumption is valid for short injection times and will provide insightful and conservative results.

Equation (1) is the one dimensional heat equation where T is the temperature at a given location; z represents the thickness direction for heat conduction to the mold; v is the velocity in the flow direction (x); q models the internal heat generation due to shear heating or crystallization kinetics, and; ρ , cp , and k are approximate thermal properties of the melt measured through laboratory instrumentation.

$$\rho c_p \left(\frac{\partial T}{\partial t} + v \frac{\partial T}{\partial x} \right) = k \frac{\partial^2 T}{\partial z^2} + q \quad (1)$$

While the heat equation has been solved numerically for the injection molding process [19], it is possible to simplify the equation further without sacrificing the value of the results in this application. For instance, let us assume the flow rates are negligible in the packing stage - this eliminates the convection and heat generation terms. Further, let us assume there are no temperature gradients across the part and the melt solidifies uniformly. Then this equation can be simplified to (2) where α is the thermal diffusivity of the melt.

$$\frac{\partial T}{\partial t} = \alpha \frac{\partial^2 T}{\partial z^2} \quad (2)$$

This equation has been solved analytically, using the Gauss error function as:

$$\frac{T(z,t) - T_{wall}}{T_{melt} - T_{wall}} = \text{erf}\left(\frac{z}{2\sqrt{\alpha t}}\right) \quad (3)$$

The purpose of this cooling model is to provide temperature data from which the specific volume of the material may be calculated with imposed cavity pressure conditions using a modified double domain Tait equation [19] as shown in equation (4). This model assumes constant density once the material has cooled below its glass transition temperature. This simplification, along with every previous assumption, produces conservative results regarding the deformation behavior of the knit-line.

$$v(T(z,t), P) = (b_1 + b_2(T - T_g)) \left(1 - C \ln \left(1 + \frac{P}{b_3 \exp(b_4(T - T_g))} \right) \right) \quad (4)$$

The derived analysis may now be used to estimate the knit-line's behavior when subjected to novel process control strategies for the material properties and molding parameters summarized in Table 2. The melt temperature and mold temperature is 280 C and 90 C, respectively. Additionally, the analysis began with the material cooling for 2.0 seconds at a cavity pressure of 30 MPa to mimic the effects of polymer skin solidification during the filling stage of injection molding.

At 2.0 seconds, one valve gate is closed while the part is packed through the other gate at 60 MPa. As the material cools across the part, volumetric shrinkage in the cavity will be replenished by material being packed through the open gate. Of particular interest, the material in the area of the part near the closed gate will experience volumetric shrinkage that will be replenished by material across the knit-line, thereby forcing the knit-

line deformation as the part solidifies. The shape of the knit-line can be calculated as a function of time considering the compressibility behavior of the polymer melt as well as the solidification of the polymer skin.

The analysis results are presented in Figure 5, which shows the movement of the knit-line through the thickness during the 2.0 seconds following the injection phase. In the Figure, the location of the knit-line at each time interval is shown by the corresponding profile. Additionally, it is necessary to track the depth of solidification where the local material temperature has dropped below the glass transition temperature and the position of the knit-line is frozen, as shown by the dark solid line in Figure 5. For example, at 2.0 seconds, the knit-line has been frozen into the part to a depth of approximately 0.1 mm due to cooling before the valve gate cycling began.

The knit-line position at the end of the filling stage is mid-way between the gates and propagates directly across the thickness, normal to the mold wall. When one gate is closed and the cavity pressure is raised to 60 MPa, the knit-line immediately bows to the position shown at time equal to 2.01 seconds, corresponding to a deflection of roughly 1.8% of the distance between the gates. This knit-line deformation is due purely to the change in the polymer's specific volume when subjected to an increase in the melt pressure. The magnitude of this movement can be increased slightly by increasing the cavity packing pressures or decreasing the cavity pressures at the end of fill before the cycling stage begins – the impact of both these strategies will be discussed later. As the polymeric material cools, moreover, significant volumetric shrinkage occurs (examine the slope of PvT data in Figure 3) which further drives the deformation and diffusion of the

knit-line. As the cooling continues, the frozen layers propagate, freezing the location of the knit-line while the knit-line continues to deform in the central molten layers.

This process is allowed to continue for a brief period of time after which all gates are reopened and the part is packed as in a conventional molding process. As shown in Figure 5, the knit-line has been dispersed across 4.8% of the distance between gates after 2.0 seconds of packing from one gate. The magnitude of the deflection can be maximized by continuing to push with one gate until the part has fully solidified. However, this processing strategy would likely result in an unbalanced cavity pressure distribution with unacceptable residual stresses and part properties. As such, experimental research was undertaken to quantify the process dynamics required to increase the structural performance of the part without simultaneously violating other product specifications.

Experimental

The application is a printer base approximately 55 cm by 35 cm with a thickness of 2.1 mm (21 x 15 x 0.085 in). The part was gated via four valve gates, which were controlled in pairs for control system simplicity. Knit-lines formed midway between the gates (30 cm apart) as shown in the geometry of Figure 6. The use of a composite material in this application was justified given the printer's mass and structural requirements. However, the decrease in knit-line strength in the conventional molding process was a potential failure mode in required impact and drop tests. Molding experiments were conducted with a 720 ton hydraulic molding machine (Mitsubishi Heavy Industries, Tokyo, Japan) and shot capacity of 115 oz. A hot manifold system (Husky Hot Runner Systems, Toronto, Canada) was utilized with timed pneumatic valve gates to control the melt flow to the cavity. To coordinate the valve gate timers with the molding machine, a

data acquisition board (National Instruments AT-MI016L-9) was used with a personal computer (Dell 486DX2/66T). At the beginning of the injection phase, the molding machine closes a relay, which signals the control system to open the valve gates and begin the control cycle.

The material under consideration is 20% glass filled, high flow polycarbonate (LEXAN™ SP7604, GE Plastics). For this material, twelve molding trials were performed in a controlled experimental design to investigate significant factors. Four variables (switch time, pack time, # cycles, and cycle duration) were examined with the levels shown in Table 3. In this process, switchover time indicates the time at which the first of the gate oscillation cycles begins. The number of push cycles indicates the number of cycles for which material is forced through alternating gates. The push time indicates the duration of time that each gate remains open before changing the gating sequence; given that this study utilized two sets of valve gates, the push time is equal to one half the period. The other molding variables represent the typical processing conditions for this material.

Once the molding cycle reached an equilibrium state, the molding experiments began. For each of the twelve experimental conditions, twelve parts were molded in succession for later tensile testing. Since none of the transient molding conditions (melt temperature, mold temperature, etc.) were changed, it was not necessary for the machine to equilibrate between molding trials.

Results and Discussion

ISO 527 Type I specimens were machined from the molded parts and equilibrated in a controlled environment of 21C and 40% relative humidity. Testing was performed on an Instron 1125 testing machine at a constant speed of 5 mm/min according to ISO 527

Method 320B for injection molded reinforced thermoplastic materials. This cross-head displacement corresponds to a strain rate of approximately 0.2 % per second. Of principle interest is the tensile stress-strain behavior of specimens across the class 1 knit-line. For reference, specimens were machined from the molded parts as shown in Figure 6. Twelve specimens from each molding condition were tested for ultimate knit-line strength. Additionally, specimens were machined and tested to determine the nominal in-flow and cross-flow tensile behavior without knit-lines.

The three curves of Figure 7 correspond to the nominal in-flow tensile properties without knit-line (solid thin line), the knit-line strength of the conventionally molded part (dashed thin line), and the tensile behavior of the knit-line molded with the described process cycle (dashed thick line). All of the parts failed in a brittle manner. The specimens containing knit-lines from conventionally molded parts behaved identical to the nominal part until a strain of 4% was reached, at which point the load carrying ability degraded and the part quickly failed. All of the conventionally molded specimens failed at the knit-lines. These results indicate that the knit-line induced a 30% loss in both elongation to failure and ultimate tensile strength - providing only 49% of the deformation energy of the nominal part.

Using the described process, the structural integrity of the specimen with knit-lines was completely restored. There are two important notes regarding the performance, moreover. First, all of the specimens molded with the described process exhibited a higher initial elastic modulus than conventionally molded specimens without knit-lines. While microscopy was not performed on the specimens, the authors believe that a higher level of fiber orientation was achieved in the load carrying direction than was previously attained

with conventional molding due to the described convective flow and increased fiber orientation. Second, the tested specimens did fail at slightly lower strains than those that were machined from conventionally molded parts. However, every one of the specimens gathered from the described process failed at the neck. On closer inspection, it was discovered that a slight discontinuity in the CNC program had induced a 0.1 mm radius stress concentration in this area.

The summary of the statistical analysis of the results from the design of experiments is listed in Table 4. The yield stress of the nominal in-flow tensile specimens was approximately 91 MPa with a standard deviation of 2.1 MPa. In conventional molding, the yield stress at the knit-lines decreased to 66.2 MPa with a standard deviation of 9.2 MPa. The loss in strength as well as increased variance are of significant concern to the product designer. With the described process, the knit-line strength was restored to its original value of ultimate tensile stress with a deviation of 2.5 MPa. In summary, the tensile properties of the knit-line can be improved in both magnitude and consistency.

To investigate the dependence of knit-line strength on a few process parameters, analysis of variance was utilized for the full set of tensile data. Four molding factors were considered, namely: switching time (varied from 1.1 to 1.65 sec), pack time (from 5.0 to 9.0 sec), number of cycles (from 1 to 8), and push time (from 6.0 to 0.25 sec). The results are shown graphically in Figure 8, which illustrates the net effect of changing each parameter individually. The width of each bar represents the 95% confidence interval of the estimate, i.e. a change in switchover time from 1.1 to 1.65 seconds will likely cause a decrease in the stress of 5 MPa with a 95% confidence that the ultimate stress of the molded specimen would decrease between 3.8 and 6.2 MPa.

The molding experiments, tensile testing, and analysis of results have established that the push time is the most important variable in improving the knit-line strength. With increased push time, more material shrinks volumetrically forcing the knit-line to disperse across a wider region - this effect is clearly shown by the analysis. A push time of 3 sec was found to be adequate for obtaining nominal part strength across the knit-line as shown in Figure 9. The switchover time is also significant since it determines the amount of solidification which has occurred before the push began and thereby limits the magnitude of the knit-line deflection. Interestingly, the number of push cycles did not significantly effect the knit-line strength. Pack time was also not found to be critical to the knit-line strength, though increased pack times might increase the knit-line strength slightly. When analyzing the results, it is useful to remember that the deviation in ultimate stress was approximately 2 MPa between molded parts, which would indicate that any factor crossing the 0 axis is insignificant.

Conclusions

In an application molded of polycarbonate with 20% short glass fibers, the ultimate yield of conventionally molded specimens with knit-lines was 70% of the nominal in-flow properties. A method for improving the knit-line properties of thermoplastic materials has been conceived, analyzed, and validated. The process relies on the compressibility and shrinkage of the polymer melt to induce flow and fiber orientation to increase the structural integrity of tensile specimens machined from molded composite parts with class 1 knit-lines. Potentially, similar or greater gains will be achieved with materials exhibiting higher losses in knit-line strength, such as polypropylene, liquid crystal polymers, and other heavily filled systems.

Testing was performed utilizing commercial tooling with a complex part geometry for examination of type 1 (butting) knit-lines only. The behavior of streaming, or transverse, knit-lines (type 2) could potentially be improved through proactive gating design and cycling gates to induce flow in orthogonal directions. For this application, streaming knit-lines could be improved by pushing the flow with one gate rather than two parallel gates (ref. Figure 6) or alternately triggering left and right gates with top and bottom gates. Importantly, the technique is extensible to different part geometries. Further analysis has shown that the magnitude of knit-line deformation is mostly independent of the thickness value, though timing becomes more critical as the wall thickness decreases. The magnitude of the knit-line deformation is proportional to the length of flow beyond the knit-line interface as shown in Figure 5. As such, gating design greatly determines the systems ability to enhance the knit-line strength.

The potential impact of this technology in composite molding applications is significant. With a simple control circuit and no tooling modifications, issues regarding the structural integrity of knit-lines may be resolved. In new applications, composite material systems, which were previously discarded due to structural concerns, may be reexamined. Moreover, this paper introduces the concept of dynamically and proactively controlling the melt flow to achieve desired fiber distributions. Ultimately, the widespread use of this and more advanced techniques could lead to new applications with stronger, thinner walled parts that were previously thought impossible.

References

- [1] R. M. Criens and H. G. Mosle: *Kunststoffe*, 1982, **72**, 222.
- [2] P. J. Cloud and F. McDowell: *Plast. Tech.*, 1976, **22**, (8), 37.
- [3] Y. C. Qu and A. Z. Yu: *Polym. Int.*, 1995, **37**, 113.
- [4] SS. B. Wilkinson and J. R. White: *Plast. Rubber Process. Appl.*, 1997, **26**, 205.
- [5] J. Z. Liang, R. K. Li, and S. C. Tjong: *Polym. Compos.*, 1997, **26**, 278.
- [6] E. Hagerman: *Plast. Eng.*, 1973, **29**, (10), 67.
- [7] N. G. McCrum, C. P. Buckley, and C. B. Bucknall: Principles of Polymer Engineering, Oxford Science Publications, New York, 1988.
- [8] K. Tomari, H. Harada, Z. Maekawa et. al.: *Poly. Eng. Sci.*, 1993, **33**, 1001.
- [9] S. G. Kim and N. P. Suh: *Poly. Eng. Sci.*, 1986, **26**, 1200.
- [10] R. S. Bay and C. L. Tucker: *Poly. Eng. Sci.*, 1992, **32**, 317.
- [11] H. Hamada, Z. Maekawa, T. Horino, K. Lee, K. Tomari: *Intern. Poly. Process.*, 1988, **29**, 131.
- [12] R. Malloy, G. Gardner, and E. Grossman: *SPE ANTEC Tech. Proc.*, 1993, **51**, 521.
- [13] W. Michaeli and S. Galuschka: *SPE ANTEC Tech. Proc.*, 1993, **51**, 534.
- [14] D. J. Dooley: *SPE ANTEC Tech. Proc.*, 1993, **51**, 414.
- [15] Garder and Cross: *Plastics Engineering*, 1993, 49, (2), 29.
- [16] Y. Termonia: *SPE ANTEC Tech. Proc.*, 1993, **51**, 296.
- [17] H. H. Chiang, C. A. Hieber, and K. K. Wang: *Poly. Eng. Sci.*, 1991, **31**, 116.
- [18] G. D. Gilmore and R. S. Spencer: *Modern Plastics*, 1950, **27**, (4).
- [19] P. Zoller: *J. Appl. Polym. Sci.*, 1979, **23**, 1051.
- [20] V. W. Wang, C. A. Hieber, and K. K. Wang: *J. of Poly. Eng.*, 1986, **7**, 21.

List of Tables and Figures

Table 1: Melt environment by process stage

Table 2: Material properties and molding conditions

Table 3: Molding variables

Table 4: Comparison of knit-line properties

Figure 1: Formation of knit-line illustrating poor adhesion, orientation, and v-notch

Figure 2: Diffusion of knit-line due to convective flow

Figure 3: Compressibility data for 20% glass filled polycarbonate

Figure 4: Melt pressure and gate cycling

Figure 5: Predicted knit-line movement after filling stage

Figure 6: Printer base with location of tensile specimens

Figure 7: Stress strain diagram for different specimens

Figure 8: Effect of process variables on ultimate stress

Figure 9: Effect of push time on ultimate stress

Table 1: Melt environment by process stage

Point	Stage	Location	Temp.	Pressure
A	Feed	Barrel	High	Low
B	Injection	Nozzle	High	High
C	Packing	Cavity	Medium	High
D	Cooling	Cavity	Lower	Lower
E	Ejection	External	Low	Low

Table 2: Material properties and molding conditions

Parameter	Value
Melt Temperature	280 C
Mold Temperature	90 C
Injection Time	1.5 sec
Cavity Pressure	30 MPa
Push Pressure	60 MPa
Push Time	5 sec
Wall Thickness	2.5 mm
Gate Distance	200 mm
Thermal Diffusivity	1 e-6
b1	0.848 cm ³ /gm
b2	5.3e-4 cm ³ /gm C
b3	2.3e9 dyne/cm ²
b4	5.5e-3 C ⁻¹

Table 3: Molding variables

Factor	Level(s)
Switchover Time (sec)	1.1, 1.65
# Push Cycles	0, 1, 2, 4, 8
Push Time (sec)	0.25, 0.66, 1.25, 2.75
Packing Time (sec)	5.00, 9.00
Injection Time (sec)	1.75
Pack Pressure (MPa)	50
Melt Temperature (°C)	270
Mold Temperature (OC)	90
Holding Time (sec)	20

Table 4: Comparison of knit-line properties

Condition	Conventional	Improved
In-Flow Ultimate Stress (MPa)	91.1 ± 2.1	
Cross-Flow Ultimate Stress (MPa)	72.0 ± 2.1	
Knit-Line Strain to Failure (%)	4.81 ± 0.6	6.11 ± 0.5
Knit-Line Ultimate Stress (MPa)	66.2 ± 9.2	92.0 ± 2.3
Knit-Line Deformation Energy (J)	5.27 ± 1.2	8.44 ± 0.8

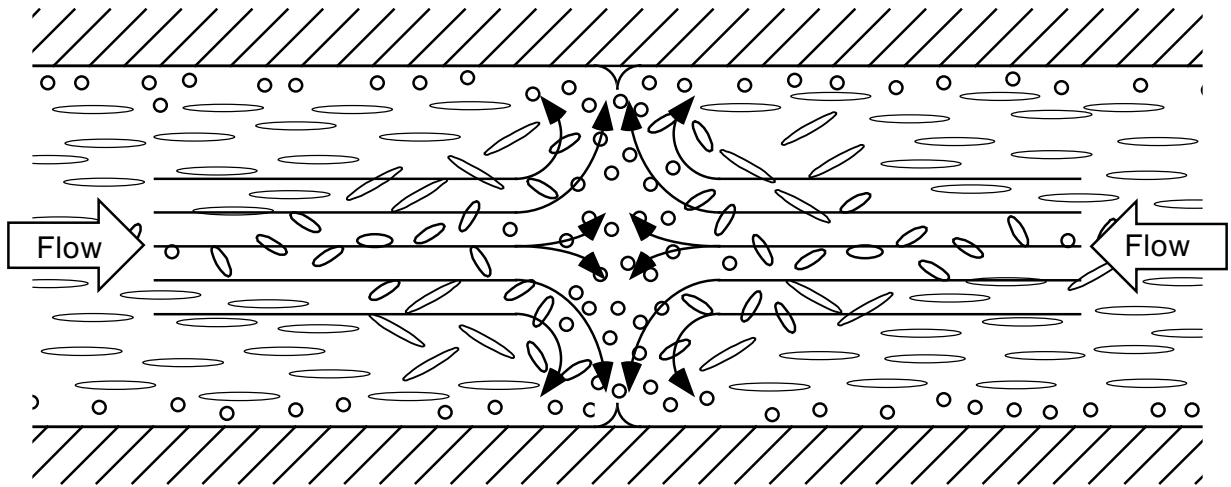


Figure 1: Formation of knit-line illustrating poor adhesion, orientation, and v-notch

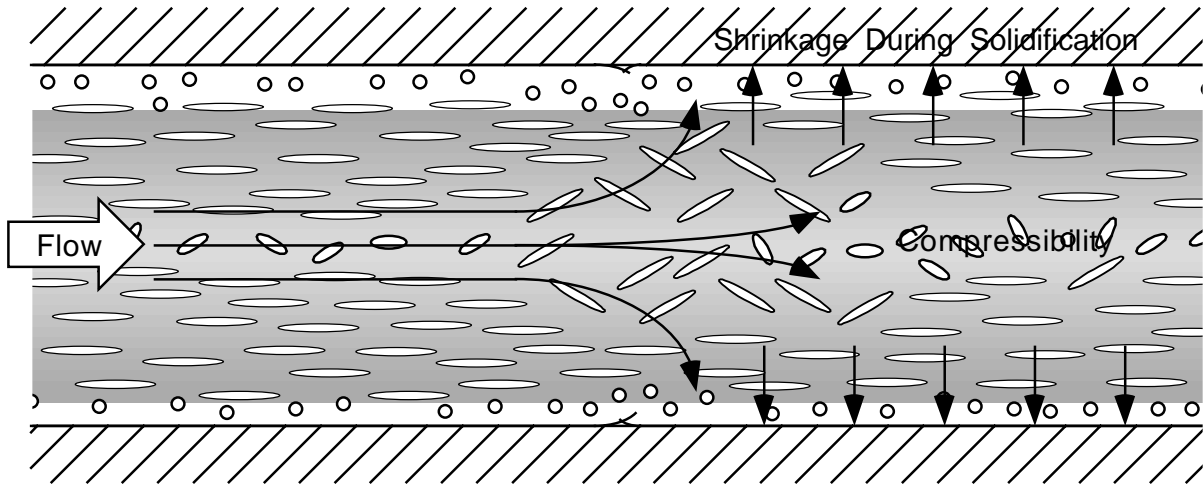


Figure 2: Diffusion of knit-line due to convective flow

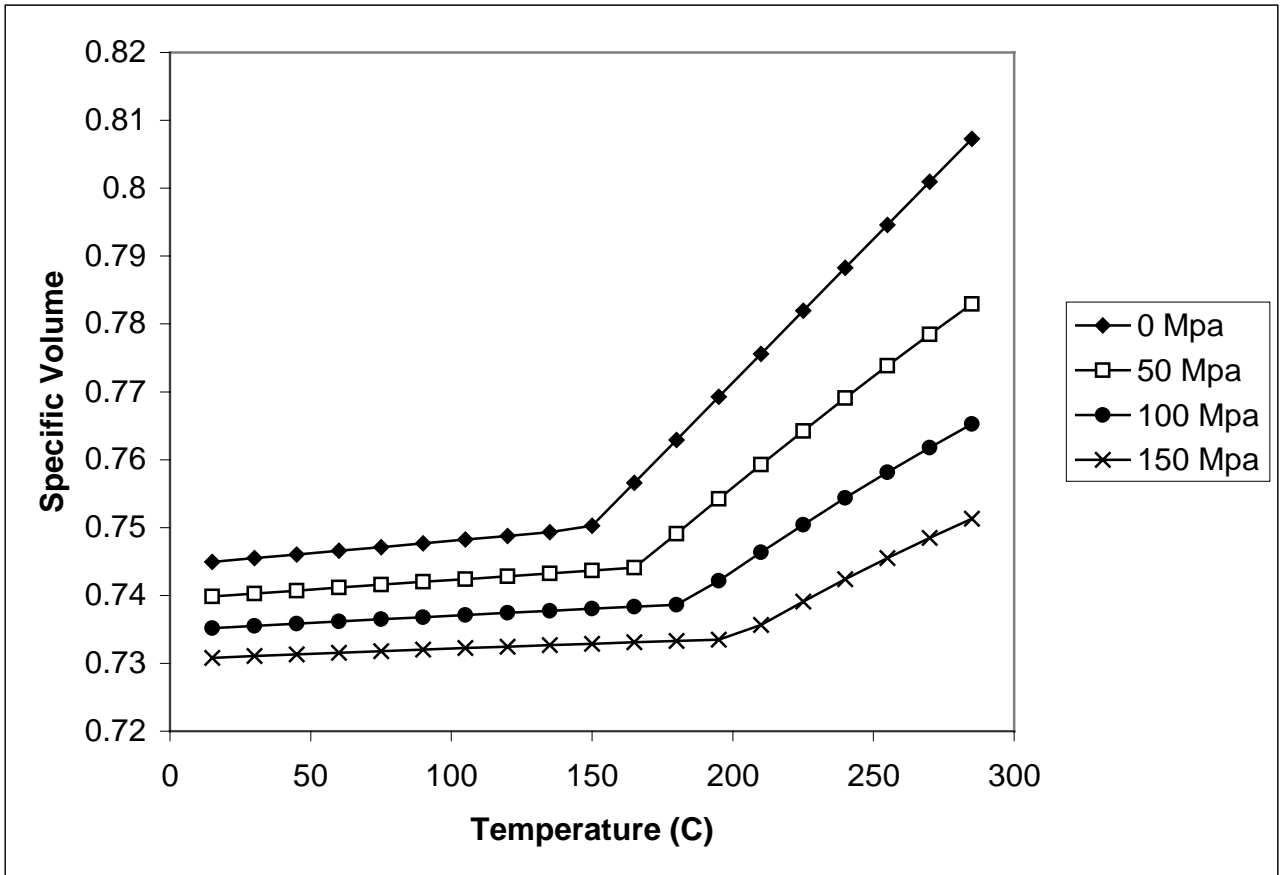


Figure 3: Compressibility data for 20% glass filled polycarbonate

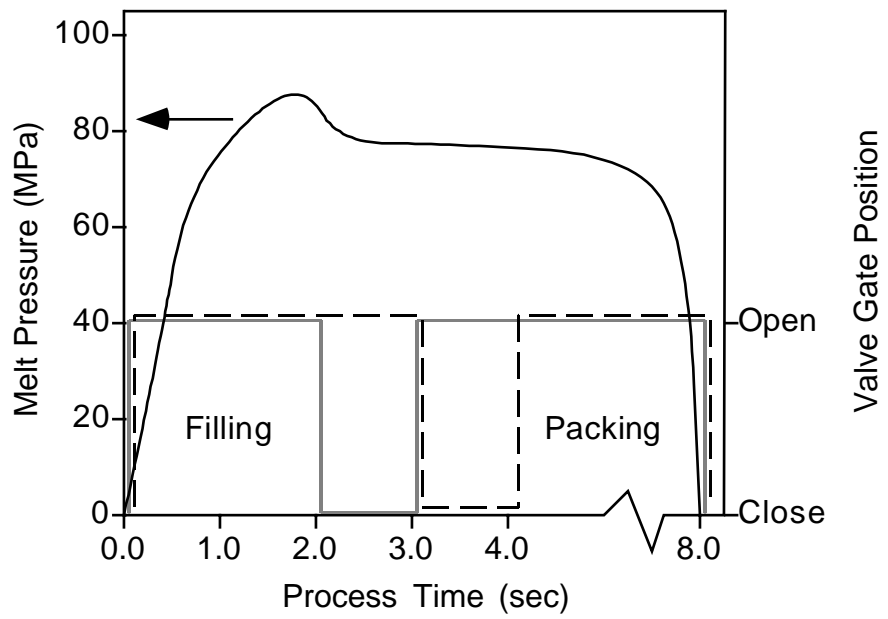


Figure 4: Melt pressure and gate cycling

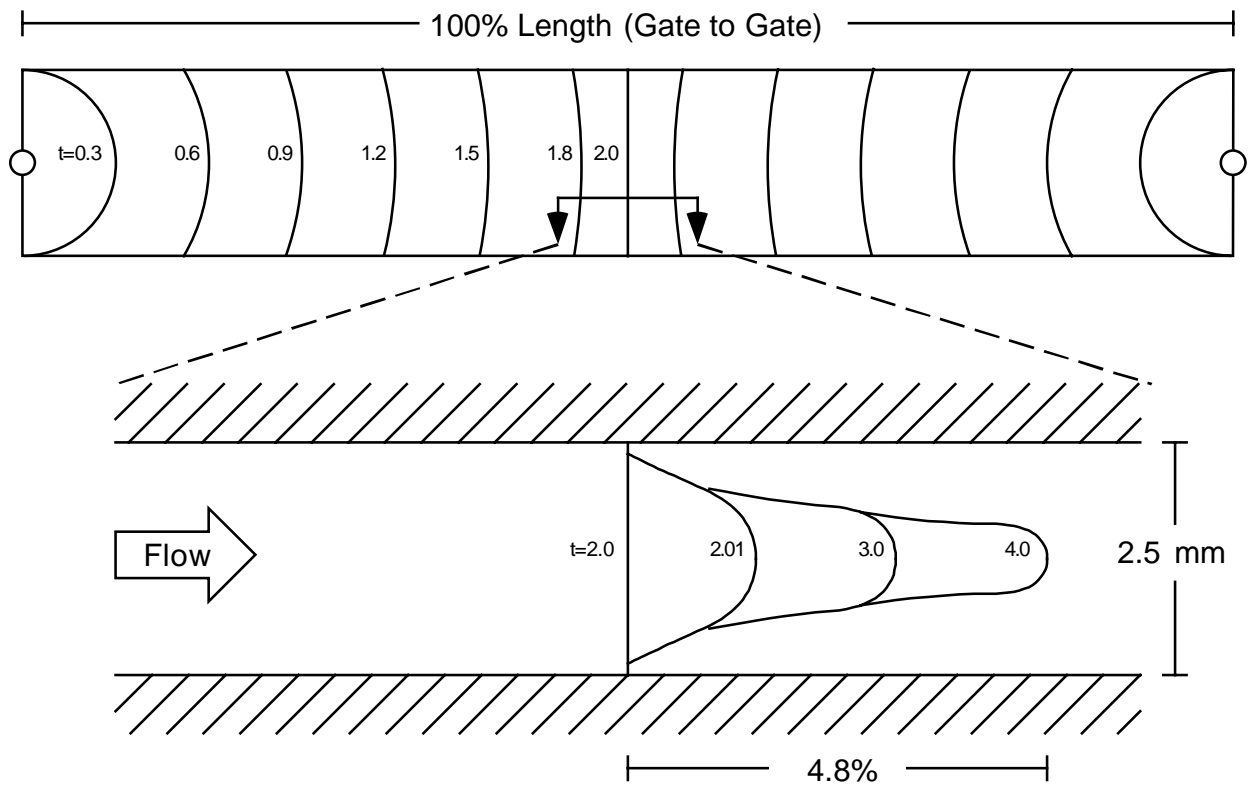


Figure 5: Predicted knit-line dispersion after filling stage

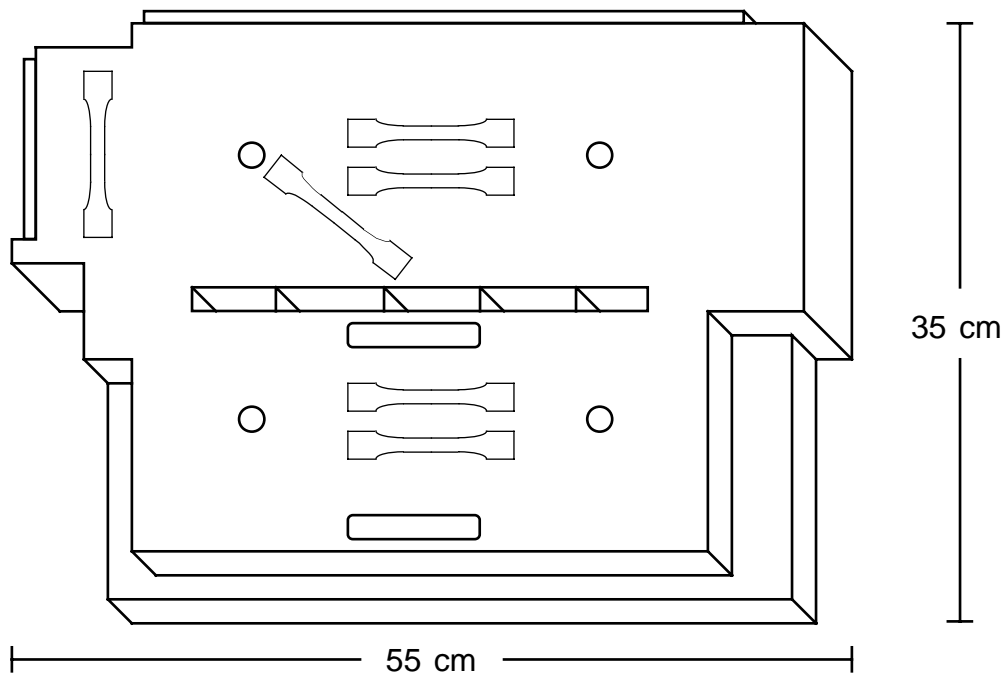


Figure 6: Printer base with location of tensile specimens

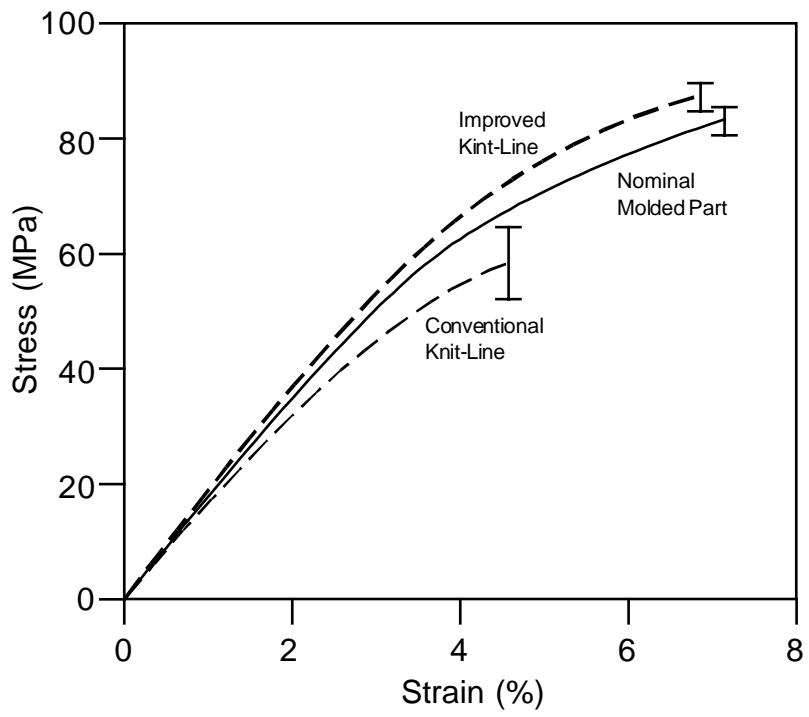


Figure 7: Stress strain diagram for different specimens

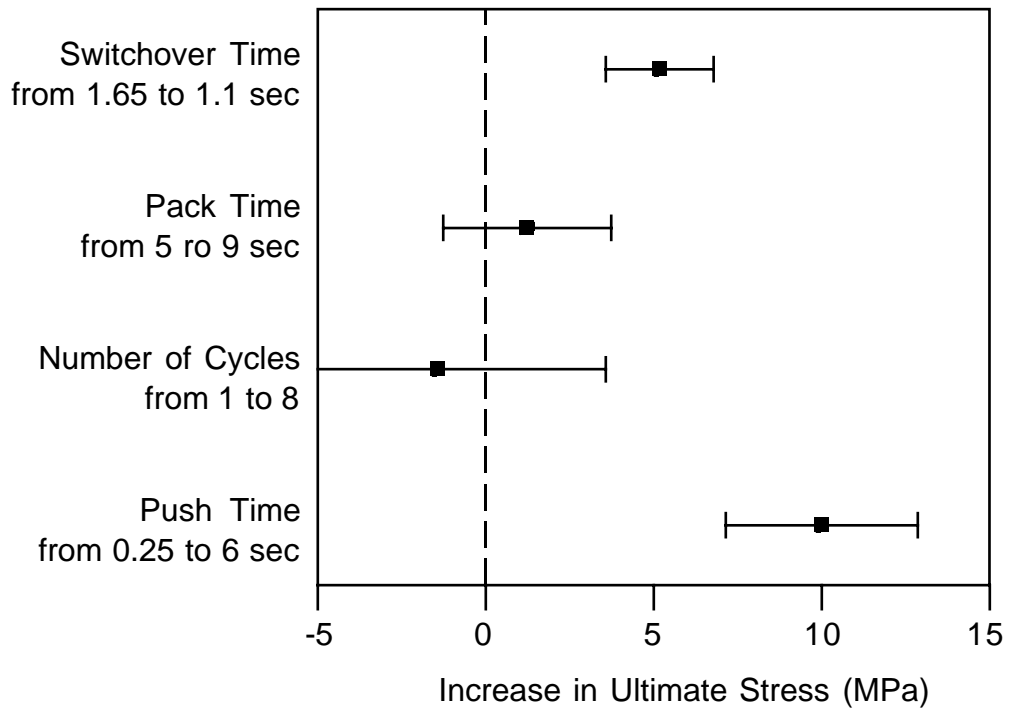


Figure 8: Effect of process variables on ultimate stress

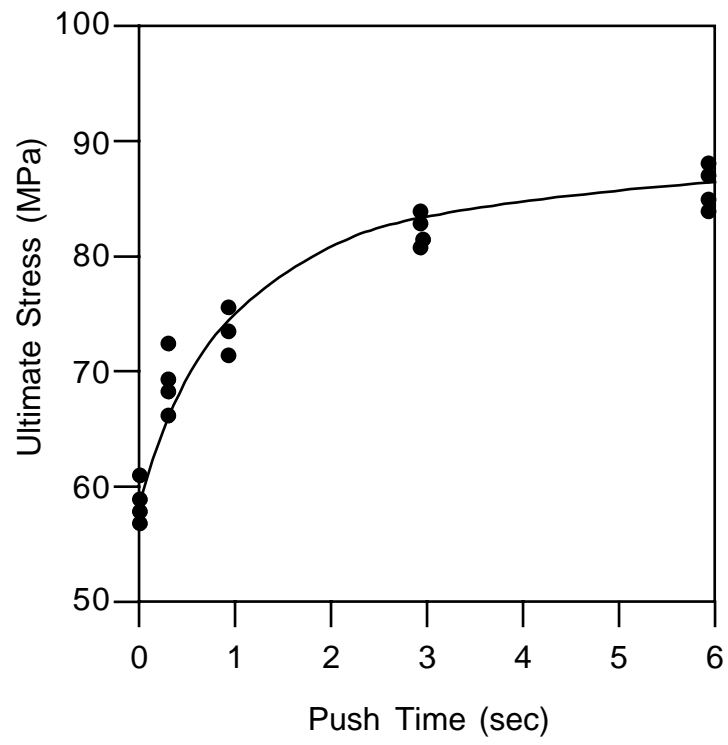


Figure 9: Effect of push time on ultimate stress